The Excluded Volume Problem in the Polymer Reference Interaction Site Model

Erik Nies,* Suxin Wang,† and Rob H. C. Janssen

Eindhoven Polymer Laboratories, Faculty of Chemical Engineering, Eindhoven University of Technology, P.O. Box 513, 5600MB Eindhoven, The Netherlands

Peter Cifra

Polymer Institute, Slovak Academy of Sciences, 842 36 Bratislava, Slovakia

Received September 18, 1997; Revised Manuscript Received November 23, 1998

ABSTRACT: An intramolecular distribution function for lattice chains, accounting for the long range excluded volume, has been derived employing an Ornstein−Zernike-like integral equation approach, initially investigated for off-lattice chains by Curro, Blatz, and Pings. The intramolecular distributions, obtained for 16-, 30-, and 60-mers, are compared to theoretical results for the freely jointed chain model and to Monte Carlo simulation data. The new single chain intramolecular distribution function accurately matches the Monte Carlo data whereas the ideal chain structure factor overestimates the short-range intramolecular correlations. Upon increasing density the simulated intramolecular distributions gradually evolve toward the ideal chain results although the latter are never actually reached. The intermolecular distributions for athermal and interacting 30-mers at several densities have been calculated by combining the investigated intramolecular distribution functions with the lattice-PRISM theory. Furthermore, the equation of state for athermal 20- and 30-mers and the liquid−vapor spinodal for 16-mers have been investigated. It is found that the ideal chain distribution function results in unphysical thermodynamic behavior, reflected in the equation of state as well as in the liquid−vapor spinodal. The predicted intermolecular distribution is quite reasonable, considering the simplicity of the ideal chain model. The combination lattice−PRISM/excluded volume intramolecular distribution function offers at least qualitatively correct results both for the thermodynamic properties and intermolecular correlations. abstract

1. Introduction

The interest in the thermodynamic behavior of polymers runs almost in parallel with the advent of polymer science. Already in the 1940s, Flory[1] and Huggins[2] independently formulated the, by now, classic Flory−Huggins (FH) expression for the free enthalpy of mixing and revealed the importance of the chain like structure for the phase behavior of polymer solutions. It was realized from the start that the FH theory was a rather crude approximation for real liquids since it is based on the lattice model.[3] For instance, it is known that packing effects typical of the dense fluid state are not captured by the lattice model. However, these packing effects have been incorporated quite early in, e.g., cell[4] and hole theories[5,6] or, more recently, by combining the FH expression with insights gained from off-lattice theories for monatomics or simple molecules.[7] Nevertheless, the simple lattice model for polymers was further refined and elaborated for, e.g., compressible lattice fluids[8] and systems involving specific interactions.[9,10]

Nowadays, many different macromolecular architectures have been synthesized, and in addition to simple linear homopolymers, well-defined branched, comb, and star polymers, block copolymers, etc. are available. These more complex materials require a more detailed description of the thermodynamic behavior in relation to their particular molecular structure. Unfortunately, such details in molecular architecture are not easily incorporated in a FH-like theory. An important advancement in lattice theories is the lattice cluster theory (LCT) designed by Freed and co-workers.[11−15] The LCT not only provided systematic improvements to the primitive FH result for linear chains but also made it feasible to study the influence of more complicated molecular structures on the thermodynamic behavior. The LCT has been successfully applied to investigate the influence of monomer structure in, e.g., mixtures of polystyrene/poly(vinyl methyl ether)[16] and mixtures of linear and short chain branched polymers.[17] Despite the developments facilitated by the LCT the major drawback of the lattice model is not alleviated.

Another line of approach, relying on the integral equation theory of monatomic and simple molecular fluids, was investigated by Curro, Schweizer, and collaborators.[18−21] Integral equation theories were initially developed for simple monatomic fluids to study the microscopic structure of dense fluids employing correlation functions. The thermodynamic properties can be derived from the correlation functions employing exact statistical mechanical relationships.[22,23] Unfortunately, and this is a major drawback of all integral equation theories, these calculations are plagued with so called thermodynamic inconsistencies which are related to the necessary approximations involved in the calculation of the theoretical correlations.[24−30]

These liquid state theories, employing correlation functions, were extended to simple molecular fluids in the reference interaction site model (RISM) theory by Chandler and co-workers.[31] The RISM theory makes it feasible to predict the intermolecular correlations among segments or interaction sites on different molecules from

† Present address: Physical and Macromolecular Chemistry, Leiden Institute of Chemistry, Gorlaeus Laboratoria, University of Leiden, Postbus 9502, 2300 RA Leiden, The Netherlands.

10.1021/ma971381c CCC: $18.00
Published on Web 02/24/1999

information of the intramolecular distributions, which are set by the molecular architecture. For simple (rigid) molecules the intramolecular distribution is known in advance and the RISM theory is quite successful in describing the subtle packing effects in dense liquids induced by the intramolecular structure. It should be noted that, in contrast with the integral equation theory for simple monatomic, the RISM calculations are not as accurate at low densities;[24,25,32] e.g., it has been shown that the RISM theory does not yield the correct ideal gas limiting behavior.[33]

The application of the RISM theory to flexible chain molecules (polymer-RISM or PRISM) was initiated by Curro and Schweizer to study the microscopic structure of polymer single components and mixtures.[18−21] For flexible macromolecules, the intramolecular structure is not *a priori* known and it must be expected to depend on the intermolecular correlations which in turn are determined by the intramolecular distribution. Hence, a complicated interdependence between inter- and intramolecular correlations exists, and in principle, both must be calculated self-consistently.[34−40] The first attempts to establish this self-consistency have been published only recently and are still a matter for further investigation.[34−40]

In the initial applications of the PRISM theory, a more simple approach was taken by assuming that the intramolecular structure was *a priori* given.[18−21] In certain instances this additional approximation turns out to be quite reasonable. In particular in the dense melt it is known from the ideality hypothesis of Flory[3,41] that the intramolecular distribution is successfully described by an ideal chain model. Typical for the ideal chain model is that the average squared end-to-end distance $\langle r^2 \rangle$ depends on the chain length s according to $\langle r^2 \rangle \sim (s-1)^1$. However, at low densities the screening of inter- and intramolecular interactions becomes less efficient and the intramolecular distribution evolves to that of a self-avoiding walk.[42] In this case the average squared end-to-end distance scales with the chain length according to $\langle r^2 \rangle \sim (s-1)^{1.2}$. Furthermore, deviations from ideal chain statistics must be expected and are known to exist in polymer mixtures.[43,44]

Nevertheless, the PRISM theory has been quite successful in predicting the intermolecular correlations starting from the intramolecular distribution. Several intramolecular distribution functions, derived from different ideal chain models and incorporating varying chemical details such as the Gaussian chain,[18−21,45] the freely jointed chain,[18−21,45] and the nonreversal random walk,[18−21,45] have been investigated. Most of these applications involved rather dense fluids, and the correlations are mainly governed by segmental packing effects which are equally active in simple molecular and monatomic fluids. In these circumstances the additional subtleties related to the chain connectivity are not that easily appreciated and, in order to study these effects, lower densities should be investigated. Unfortunately at lower densities, irrespective of the ideality assumption necessary for chainlike molecules, it is known that the PRISM approach becomes less accurate.[24,25,32,33]

In order to make a systematic study of these chain connectivity effects possible, previous research in our laboratory applied the (P)RISM theory to the lattice model.[22] At first sight this approach might seem counterintuitive or even counterproductive. Integral theories were precisely developed to study the intricacies of the continuum that are not captured by the lattice model. However, a few practical advantages of the lattice model immediately become obvious. First, the actual calculation of lattice correlation functions is significantly easier than the calculation of the off-lattice correlations.[22,46] Second, molecular simulation techniques, in particular Monte Carlo simulations, are also much easier and more efficient on-lattice than off-lattice.[18−22,46] It is well-known that molecular simulations provide essentially exact information for the investigated model.[42] Hence, the more efficient lattice simulations can provide more information and make a more extensive comparison amenable.

Apart from these practical advantages, more fundamental reasons can be thought of as well. As already mentioned in a previous paragraph, the overwhelming off-lattice packing effects, which are very similar for monatomic, simple fluids and polymeric fluids, are absent on the lattice. This makes a more detailed study of chain connectivity effects feasible, even at high densities where the PRISM theory is expected to be at its best.

Furthermore, it has already been shown that the effects of theoretical approximations can be studied equally well on the lattice. For instance, the peculiarities of the Percus−Yevick (PY) theory for the sticky sphere[47,48] model of Baxter are also found on the lattice.[22] Therefore, it may be expected that the effects of chain connectivity, operating on length scales larger than the lattice spacing, will be equally present on the lattice as in off-lattice models.

As mentioned previously, most applications of PRISM theory involved ideal chain structure factors. All these models fail to incorporate the long range correlations resulting from the excluded volume present in chain molecules.[18−21] As a result these intramolecular distribution functions include unphysical overlaps of chain segments.[18−21] It is known that these intramolecular overlaps especially have a profound influence on the thermodynamic properties of the polymer fluid.[18−21] This has been shown on several occasions, both off-lattice[18−21] and on-lattice.[22] To correct for this overlap it was suggested to correct the intramolecular distribution function *ad hoc* but to keep at the same time the overall ideal chain behavior.[18−22]

In the present work we assume, in line with previous work on the PRISM theory, the intramolecular distribution as *a priori* given and investigate a single chain intramolecular distribution function which accounts for the excluded volume. The present development, invoking a finite difference integral equation for the isolated chain, was previously investigated by Curro, Blatz, and Pings for an athermal off-lattice polymer chain.[49] This new intramolecular distribution function is then injected in the PRISM theory and the influence on the intermolecular correlations and the thermodynamic properties is examined at both high and low densities. In the second paragraph the lattice PRISM theory and several frequently used intramolecular distribution functions are discussed. In addition the new excluded volume intramolecular distribution function is introduced and finally the routes to the thermodynamic properties discussed in this work are presented. The theoretical results are compared to Monte Carlo simulation results and evaluated in section 4. The simulation algorithms have been presented previously.[50] Hence, only the most important aspects are summarized in section 3. Finally,

in the concluding section the main results are recapitulated and related consequences are summarized.

2. Theory

2.1. The Molecular Model. Consider N linear s-mers each of which occupies s consecutive sites on a cubic lattice of N_L sites, each of volume v^*. The overall fraction of filled lattice sites or the segmental packing fraction, y, is given by

$$y = sN/N_L \tag{1}$$

Noncovalently bonded polymer segments i and j are assigned a nearest neighbor interaction potential, $u_{ij}(l,m,n) = u(l,m,n)$

$$u(l,m,n) = \begin{cases} \infty, & l^2 + m^2 + n^2 = 0 \\ u_{attr}, & l^2 + m^2 + n^2 = 1 \\ 0, & \text{otherwise} \end{cases} \tag{2}$$

The covalent bonds between consecutive segments i and $i + 1$ can be represented by the following pair potential, $w_{ii+1}(l,m,n) = w(l,m,n)$

$$w(l,m,n) \rightarrow +\infty, \quad l^2 + m^2 + n^2 \neq 1 \tag{3a}$$

$$w(l,m,n) = 0, \quad l^2 + m^2 + n^2 = 1 \tag{3b}$$

where $\beta = 1/(k_B T)$, δ is the Kronecker delta function, and the position of the second segment relative to the first one is given by the lattice indices (l,m,n); each index can attain the values 0, ±1, ±2, ...

2.2. Lattice PRISM Theory. A successful theoretical route to the intermolecular correlations in simple atomic fluids is given by the Ornstein−Zernike integral equation. The OZ integral equation was generalized by Chandler and co-workers to molecular fluids with a given intramolecular structure. Here we only consider homogeneous systems for which all correlation functions are translationally invariant and, hence, are only functions of the relative distance between segments. If the total intermolecular pair correlation function, $h_{ij}(l,m,n)$, between the pair of segments i and j is considered to propagate in a sequential manner by direct intermolecular correlation $c_{ij}(l,m,n)$ and intramolecular distribution $\omega_{ij}^{intr}(l,m,n)$, the Fourier transform of the generalized Ornstein−Zernike matrix equation on a cubic lattice can be written as[18−21,31,51]

$$\hat{H}(k_l,k_m,k_n) = \hat{\Omega}(k_l,k_m,k_n)\hat{C}(k_l,k_m,k_n) \times \left[\hat{\Omega}(k_l,k_m,k_n) + \frac{y}{s}\hat{H}(k_l,k_m,k_n)\right] \tag{4}$$

where the circumflex denotes Fourier transformation and (k_l,k_m,k_n) are the Fourier variables conjugate to (l,m,n); $\hat{H}(k_l,k_m,k_n)$, $\hat{C}(k_l,k_m,k_n)$, and $\hat{\Omega}(k_l,k_m,k_n)$ are $s \times s$ matrices with elements $\hat{h}_{ij}(k_l,k_m,k_n)$, $\hat{c}_{ij}(k_l,k_m,k_n)$, and $\hat{\omega}_{ij}^{intr}(k_l,k_m,k_n)$, respectively (the lattice Fourier transform is defined in Appendix A by eq A12). For instance, the $s \times s$ matrix $\hat{H}(k_l,k_m,k_n)$ is given by

$$\hat{H}(k_l,k_m,k_n) = \begin{vmatrix} \hat{h}_{11} & \dots & \hat{h}_{1s} \\ \vdots & \ddots & \vdots \\ \hat{h}_{s1} & \dots & \hat{h}_{ss} \end{vmatrix} (k_l,k_m,k_n) \tag{5}$$

The direct correlation function and intramolecular distribution are given by similar matrices $\hat{C}(k_l,k_m,k_n)$ and $\hat{\Omega}(k_l,k_m,k_n)$.

For linear s-mers this matrix equation, eq 4, becomes virtually impossible to handle. Fortunately, as shown by Curro and Schweizer,[52] eq 4 can be simplified substantially if one realizes that for sufficiently long chain molecules $\sum_j \hat{h}_{ij}(k_l,k_m,k_n)$, $\sum_j \hat{c}_{ij}(k_l,k_m,k_n)$, and $\sum_j \hat{\omega}_{ij}^{intr}(k_l,k_m,k_n)$ are virtually independent of i.[52] Hence, $\hat{h}(k_l,k_m,k_n) = (1/s^2)\sum_i\sum_j \hat{h}_{ij}(k_l,k_m,k_n)$ and $\hat{c}(k_l,k_m,k_n) = (1/s^2)\sum_j\sum_i \hat{c}_{ij}(k_l,k_m,k_n)$ are site index independent and the matrix equation can be reduced to a single algebraic equation for the intermolecular correlations

$$\hat{h}(k_l,k_m,k_n) = \hat{\omega}^{intr}(k_l,k_m,k_n)\hat{c}(k_l,k_m,k_n) \times [\hat{\omega}^{intr}(k_l,k_m,k_n) + y\hat{h}(k_l,k_m,k_n)] \tag{6}$$

where the average intramolecular two-segment distribution function $\hat{\omega}^{intr}(k_l,k_m,k_n)$ is defined as

$$\hat{\omega}^{intr}(k_l,k_m,k_n) = \frac{1}{s}\sum_{i=1}^{s}\sum_{j=1}^{s}\hat{\omega}_{ij}^{intr}(k_l,k_m,k_n) \tag{7}$$

In order to solve the equation, eq 6, for the intermolecular segmental correlations given $\hat{\omega}$ we need another relation between $h(l,m,n)$ and $c(l,m,n)$. Only approximate relations such as the PY and MSA closures are available. The closure used here is the MSA approximation given by[53]

$$h(0,0,0) = -1 \tag{8a}$$

$$c(l,m,n) = \begin{cases} -\beta u_{attr}, & l^2 + m^2 + n^2 = 1 \\ 0, & \text{otherwise} \end{cases} \tag{8b}$$

For athermal conditions, the PY and MSA approximations are identical. In both of the closures, the condition on the intermolecular pair correlation $h(0,0,0)$ is exact whereas the conditions for the direct correlations are approximate. It is known from the study of monatomic particles that the PY closure is less suited to obtain the thermodynamic properties of interacting systems.[22,47,48] Henceforth, for systems involving attractive nearest neighbor interaction energies we only consider the MSA closure.

In addition to the closure relation an expression for the intramolecular distribution function is required. The choices for $\hat{\omega}^{intr}(k_l,k_m,k_n)$ employed in this investigation will be discussed in the next subsections. Combining eqs 6 and 8 and an expression for the intramolecular distribution, eq 7, the intermolecular correlations of the lattice fluid can be calculated.

2.3. Intramolecular Distribution of the Freely Jointed Chain Model. For a chain molecule in its own melt, we may resort to the ideality hypothesis put forward by Flory. It is well accepted that due to the screening of inter- and intramolecular interactions the inter- and intramolecular correlations of a chain molecule in its own melt are effectively similar to those of an ideal chain. Flory's idea has been proven fundamentally correct by neutron scattering experiments on labeled chains[54,55] and by computer simulations.[56,57] Invoking the ideality assumption the intramolecular distribution function can be calculated independently and the results serve as input in the integral equation. Several ideal chain models with varying chemical

details have been tested, e.g., the Gaussian chain,[18−21] the freely jointed chain,[18−21] the rotational isomeric state model,[18−21] etc. The freely jointed chain has been used in previous studies[22] and will serve here as a reference. It must be pointed out that the ideality hypothesis will be particularly useful in the dense state. However, at lower densities the screening between inter- and intramolecular interaction is no longer complete, and the intramolecular distribution will tend to that of a self-avoiding walk.

The intramolecular distribution of the ideal chain model can be described solely in terms of the 1-bond-jump probability $\tau(l,m,n)$, on the cubic lattice, given by

$$\tau(l,m,n) = \begin{cases} \frac{1}{6}, & l^2 + m^2 + n^2 = 1 \\ 0, & \text{otherwise} \end{cases} \tag{9}$$

In the case of the freely jointed chain model the summation in eq 7 can be performed explicitly and the intramolecular distribution function can be shown to be given by[20−22]

$$\hat{\omega}_{\mathrm{id}}^{\mathrm{intr}}(k_l,k_m,k_n) = \frac{1 - \hat{\tau}^2 - \frac{2}{s}\hat{\tau} + \frac{2}{s}\hat{\tau}^{s+1}}{(1-\hat{\tau})^2} \tag{10}$$

where $\hat{\tau} = \hat{\tau}(k_l,k_m,k_n) = \phi/3$ and $\phi = [\cos(k_l) + \cos(k_m) + \cos(k_n)]$.

The intramolecular distribution function given in eq 10 can be used as the input for eq 6 of the PRISM theory. It is analogous to its continuum version,[18,58] and the derivation is given elsewhere.[22,59]

In the freely jointed chain model unphysical intramolecular overlaps are possible. Thus, some thermodynamic properties of athermal and interacting polymers obtained from this kind of ideal chain model are expected to be inadequate or unphysical. In order to investigate the influence of the intramolecular distribution function on the thermodynamic properties, an alternative single chain molecule model, accounting for the intramolecular short and long range excluded volumes is investigated.

2.4. Intramolecular Distribution of Excluded Volume Theory. For the off-lattice single chain in vacuum the excluded volume was discussed by Curro, Blatz, and Pings (CBP) starting from the distribution function for the chain ends.[49] Employing a diagrammatic analysis, similar to that leading to the OZ equation of a simple fluid, a $(N-1)$th-order integro-differential equation for the end point distribution function was derived. Here we extend this method to the cubic lattice and in addition calculate the intramolecular distribution function. Just as in conventional liquid state theory of simple fluids, this integro-differential equation can only be solved provided an additional closure relation is introduced. Following CBP, the analogue of the PY closure is adopted. A detailed description of the theoretical considerations is given in Appendix A.

Here we summarize the results applicable to an athermal chain with intramolecular segmental interactions given by eqs 2 and 3 at $u_{\mathrm{attr}} = 0$. In particular, the Fourier transform of the intramolecular two-segment distribution function $\hat{\omega}_{ij}^{\mathrm{intr}}(k_l,k_m,k_n)$ of a chain consisting of s segments is given by[49]

$$\hat{\omega}_{ij}^{\mathrm{intr}}(k_l,k_m,k_n) = \frac{\hat{t}_{ij}(k_l,k_m,k_n) - t_{ij}(0,0,0)}{\hat{t}_{ij}(0,0,0) - t_{ij}(0,0,0)} \tag{11a}$$

$$t_{ij}(l,m,n) = \left(\frac{1}{2\pi}\right)^3 \int_{-\pi}^{\pi}\int_{-\pi}^{\pi}\int_{-\pi}^{\pi} \hat{t}_{ij}(k_l,k_m,k_n)\cos(lk_l) \times \cos(mk_m)\cos(nk_n)\,\mathrm{d}k_l\,\mathrm{d}k_m\,\mathrm{d}k_n \tag{11b}$$

The functions $\hat{t}_{ij}(k_l,k_m,k_n)$ can be obtained from the recurrent formula

$$\hat{t}_{12}(k_l,k_m,k_n) = 2\phi \tag{12a}$$

$$\hat{t}_{ij}(k_l,k_m,k_n) = 2\phi[\hat{t}_{ij-1}(k_l,k_m,k_n) - t_{i+1j}(0,0,0) - t_{ij-1}(0,0,0)] - \sum_{k=3}^{s-2} t_{1k}(0,0,0)[\hat{t}_{ks}(k_l,k_m,k_n) - t_{ks}(0,0,0)] \tag{12b}$$

Thus, to calculate the terms $\hat{\omega}_{ij}^{\mathrm{intr}}(k_l,k_m,k_n)$, the corresponding $\hat{t}_{ij}(k_l,k_m,k_n)$ are required. These can be calculated in sequence starting from $\hat{t}_{ij}(k_l,k_m,k_n) = \hat{t}_{12}(k_l,k_m,k_n)$. The functions $t_{ij}(0,0,0)$ appearing in eq 11a are obtained from $\hat{t}_{ij}(k_l,k_m,k_n)$ by inverse Fourier transformation (eq 11b). For short s-mers ($s \le 6$), the required factors $\hat{t}_{ij}(k_l,k_m,k_n)$ and corresponding segmental intramolecular distributions $\hat{\omega}_{ij}^{\mathrm{intr}}(k_l,k_m,k_n)$ are summarized in Table 1. Further explicit summation according to eq 7 leads to the average two-segment intramolecular distribution function $\hat{\omega}_{\mathrm{excl}}^{\mathrm{intr}}(k_l,k_m,k_n)$ that can be written as a polynomial in the variable (2ϕ)

$$\hat{\omega}_{\mathrm{excl}}^{\mathrm{intr}}(k_l,k_m,k_n) = \sum_{i=0}^{s-1} c_i^s (2\phi)^i \tag{13}$$

the coefficients c_i^s for short s-mers ($s \le 6$) are given in Table 2.

The intramolecular distribution function eq 13 can be used as input to the PRISM integral theory. In the derivation of eqs 11 and 12 an approximation analogous to the Percus−Yevick approximation has been used. For continuum fluids, it has been shown that the calculated average end-to-end distance for athermal chains is larger than the exact value. For example, the exact and calculated values of the mean-square end-to-end dis-

Table 1. Segmental Intramolecular Distribution $\hat{\omega}_{ij}^{\mathrm{intr}}(k_l,k_m,k_n)$ and the t_{ij}'s for s-mers, $s \le 6$

i,j	$\hat{t}_{ij}(k_l,k_m,k_n)$	$\hat{t}_{ij}(0,0,0)]$	$t_{ij}(0,0,0)]$	$\hat{\omega}_{ij}^{\mathrm{intr}}(k_l,k_m,k_n)$
1,2	2ϕ	6	0	$\phi/3$
1,3	$(2\phi)^2$	36	6	$((2\phi)^2 - 6)/30$
1,4	$(2\phi)^3 - 24\phi$	144	0	$((2\phi)^3 - 12(2\phi))/144$
1,5	$(2\phi)^4 - 18(2\phi)^2 + 36$	684	18	$((2\phi)^4 - 18(2\phi)^2 + 18)/666$
1,6	$(2\phi)^5 - 24(2\phi)^3 + 72(2\phi)$	3024	0	$((2\phi)^5 - 24(2\phi)^3 + 72(2\phi))/3024$

Table 2. Coefficients for the Average Intramolecular Segmental Distribution Function for s-mers, $s \le 6$

s	c_0^s	c_1^s	c_2^s	c_3^s	c_4^s	c_5^s
2	1	1/6				
3	13/15	2/9	2/90			
4	4/5	5/24	1/30	1/288		
5	2139/2775	1/5	243/8325	1/180	1/1665	
6	3753/4995	5508/27216	396/14985	117/27216	1/999	1/9072

tances for off-lattice athermal 4-mers are $\langle r_{14}^2\rangle = 4.31 l_b^2$ and $\langle r_{14}^2\rangle = 4.5 l_b^2$, respectively.[49] However, despite this discrepancy that increases with increasing chain length, the local distribution around each segment is well captured by eq 13. We believe that this is the reason for the success of eq 13 (see section 4).

2.5. Thermodynamic Properties. Once the correlation functions are known, the thermodynamic properties can be calculated from exact statistical mechanical relations. The isothermal compressibility which is defined as

$$\kappa_T = -\frac{1}{V}\left(\frac{\partial V}{\partial p}\right)_{T,N} = \frac{1}{y}\left(\frac{\partial y}{\partial p}\right)_{T,V} \tag{14}$$

can be found from the zero wave vector limit of the structure factor $\hat{S}(0,0,0)$, and it can be related to the correlations in the fluid[18−22] via

$$\frac{\kappa_T}{v^*} = \frac{\beta\hat{S}(0)}{y} = \frac{\beta\hat{\omega}^{\mathrm{intr}}(0,0,0)}{y[1-\hat{\omega}^{\mathrm{intr}}(0,0,0)y\hat{c}(0,0,0)]} \tag{15}$$

Equation 15 can be rewritten in terms of the total two-segment distribution function $G(l,m,n)$ according to

$$\frac{\kappa_T}{v^*\beta} = \sum_{l,m,n}[G(l,m,n)-1] \tag{16}$$

with $yG(l,m,n) = \omega^{\mathrm{intr}}(l,m,n) + yg(l,m,n)$ denoting the total density of segments at position (l,m,n) from a chosen particle, and $g(l,m,n) = h(l,m,n) + 1$ is the radial distribution function. The equation of state can be obtained from the inverse isothermal compressibility by direct integration

$$\beta P v^* = \int_0^y \left[\frac{1}{\hat{\omega}^{\mathrm{intr}}(0,0,0)} - y'\hat{c}(0,0,0)\right] \mathrm{d}y' \tag{17}$$

This equation of state is the thermal compressibility equation of state. It is fully determined by the total two-segment distribution function $G(l,m,n)$.[22]

Other possible routes to the equation of state are, e.g., *the energy equation*, *the virial equation*, and *the wall equation of state*.[22−30,60] If the calculated distribution functions were exact, the equations of state obtained from these different routes would be identical. However, the approximate closures make the results depend on the chosen route. Here we use the compressibility route to the equation of state. It is known that the PRISM equation does not yield the correct limiting low density behavior, and this will have its consequence for the integration to be conducted in eq 17.[61] Off-lattice studies pointed out that the compressibility equation of state underestimates the compressibility factor whereas the virial equation of state results in an overestimation.[61] It was further shown that the wall equation of state produced results which were believed to be nearest to the true behavior.[61] However, in a lattice study it was shown that the wall equation of state was by no means in good agreement with MC simulation data, and in this case the compressibility equation of state was in better agreement.[61] Irrespective of which route to select, it is generally accepted that the calculation of thermodynamic properties, such as the equation of state with integral equation theory, meets always with great difficulties.

To calculate the pressure via eq 17, the intra- and intermolecular correlation functions, $\hat{\omega}^{\mathrm{intr}}(k_l,k_m,k_n)$ and $\hat{c}(k_l,k_m,k_n)$, must be calculated for each y'. The numerical integration can altogether be prevented in some cases. For atomic fluids, Baxter performed the integration analytically employing the PY closure. If it is assumed that the intramolecular distribution function is independent of density, Baxter's approach can be extended to the PRISM theory. The compressibility equation of state for chain molecules then is[62]

$$\beta P v^* = \frac{y}{s} + \frac{y^2}{2}\left[-2c(0,0,0) + 6c(1,0,0)\left(\frac{c(1,0,0)}{1-\mathrm{e}^{\beta u_{\mathrm{attr}}}} - 2\right)\right] + \left(\frac{1}{2\pi}\right)^3 \int_{-\pi}^{\pi}\int_{-\pi}^{\pi}\int_{-\pi}^{\pi} (y\hat{\omega}^{\mathrm{intr}}(k_l,k_m,k_n)\hat{c}(k_l,k_m,k_n) + \ln(1 - y\hat{\omega}^{\mathrm{intr}}(k_l,k_m,k_n)\hat{c}(k_l,k_m,k_n)))\, \mathrm{d}k_l\, \mathrm{d}k_m\, \mathrm{d}k_n \tag{18}$$

Although, eq 18 was initially derived using the PY closure, it is applicable to athermal systems studied in the MSA approximation since then the MSA and PY closures are identical. Hence, numerical integration according to eq 17 is only necessary for systems with a nonzero nearest neighbor interaction potential when the MSA closure is used.

In the PV plane of a one-component fluid three regions, i.e. a stable, a metastable, and an unstable region, can be defined. In the stable region, a fluid always remains in the one phase, and in the unstable region the fluid will always separate into two phases. On the other hand, a metastable fluid is stable with respect to small density fluctuations, but large fluctuations, i.e. the formation of critical nuclei, will cause phase separation. These three regions are separated by two lines, i.e., the binodal and spinodal curves. The liquid−gas binodal defines the coexistence between a liquid and a vapor phase and delineates the stable and metastable regions. At the spinodal curve, separating the metastable and unstable regions, the compressibility diverges, i.e. $\kappa_T \to \infty$ which corresponds to the following condition

$$\frac{1}{\hat{\omega}^{\mathrm{intr}}(0,0,0)} - y\hat{c}(0,0,0) = 0 \tag{19}$$

It is known from the study of monatomic particles that the PY closure is less suited for interacting systems.[22,47,48] Therefore, in this case only the MSA closure is discussed.

3. Monte Carlo Simulation

3.1. *NpT* Simulation. The NpT ensemble simulation technique used here to obtain the equation of state data for $s = 20$, 30, and 60 athermal chains has been described elsewhere.[50] These simulations are operated in the NpT ensemble. The self-avoiding lattice chains are placed on a cubic lattice, and each site is occupied at most once. A rectangular section of a cubic lattice with a wall is used here with 50 sites in the l direction, perpendicular to the wall, and 22 sites in the other two directions. The solid wall is placed at $l = 1$ position, and 200−500 chains are put in the rectangular section. Periodic boundary conditions are used in the m and n directions. A finite pressure is exerted by changing the total volume. The necessary volume fluctuations are created by building/destroying a solid piston scanning site-by-site with respect to the solid wall. The configu-

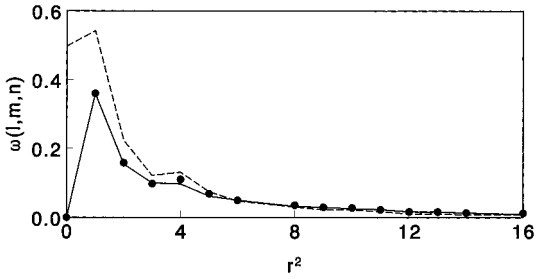

Figure 1. Intramolecular distribution function $\omega^{intr}(r)$ for 16-mers as a function of radial distance r^2 between two segments: MC simulations (●). Full lines represent the $\omega^{intr}(r)$ from the excluded volume theory; dashed lines refer to the freely jointed chain model.

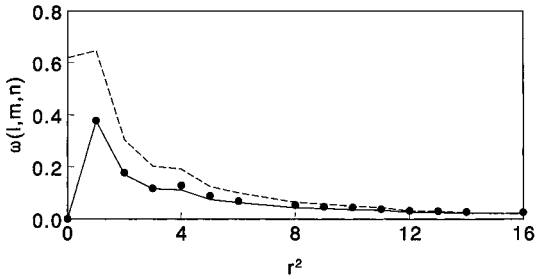

Figure 2. Caption as in Figure 1, but for for 30-mers.

ration space is sampled by moving the polymer molecules on the lattice with reptation moves. A volume fluctuation move was applied every 200 reptations. Up to 1.2×10^9 reptation moves were used, from which the first $(0.4-0.6) \times 10^9$ were used only for the equilibration of each state. The particle distributions were only obtained from the last 0.1×10^9 moves. Averages of $g_{MC}(l,m,n)$ and $\omega^{intr}_{MC}(l,m,n)$ were collected every 5000 reptations from a middle section of the polymer slab, at least seven sites away from the solid wall and from the jagged edge of the piston. The $g_{MC}(l,m,n)$ and $\omega^{intr}_{MC}(l,m,n)$ were only obtained for $r^2 = l^2 + m^2 + n^2 \leq 16$. The single chain intramolecular distribution data are obtained from the same simulation algorithm at very low concentration of chains.

3.2. Liquid−Vapor Coexistence Curve. The MC simulation data for the liquid−vapor binodal curve is taken from recent papers of Yan et al.[63,64] The phase-equilibrium coexistence curve is extracted from a new simulation algorithm, i.e., the configurational-bias-vaporization method, which is designed for studying phase equilibria for lattice polymers. A single simulation cell is used in this method where all polymers are introduced in the lower portion of the cell upon initiation. Vaporization is then carried out by randomly eliminating a chain followed by generating a new chain through the configurational-bias method.[42] The compositions of coexistence phases are determined directly. The phase-equilibrium coexistence curves for polymer systems with chain length up to 200 can be obtained from this simulation.

4. Results and Discussions

In Figures 1−3 theoretical and simulation results for the average intramolecular distribution function of 16-, 30-, and 60-mers are presented as a function of $r^2 = l^2 + m^2 + n^2$, the radial distance between two segments. The symbols (●) are single chain MC simulation data and theoretical intramolecular distribution functions $\omega^{intr}(l,m,n)$ are denoted by lines: the dashed line refers to the freely jointed chain, and the solid line depicts the excluded volume chain. To focus on the interesting part of the intramolecular distribution the trivial self correlation at the (0,0,0) position is not depicted, i.e. at the origin $\omega^{intr}(0,0,0) - 1$ is shown, whereas for all other positions, $(l,m,n) \neq (0,0,0)$, the complete intramolecular distribution $\omega^{intr}(l,m,n)$ is presented. In agreement with the simulation data the theoretical $\omega^{intr}(l,m,n)$ is only defined at lattice positions and the lines are merely a convenient manner to distinguish the theoretical results from the simulation data. The larger value for the intramolecular distribution function at $r^2 = 4$ compared to the value at $r^2 = 3$ is governed by the possible molecular arrangements on the cubic lattice. The cubic lattice also dictates that we find slightly different values for, e.g., $\omega^{intr}(2,2,1)$ and $\omega^{intr}(3,0,0)$, although both positions represent the same radial distance. Therefore, the value of $\omega^{intr}(9)$ in Figures 1−3 is obtained as the average involving the different lattice positions with the same radial distance.

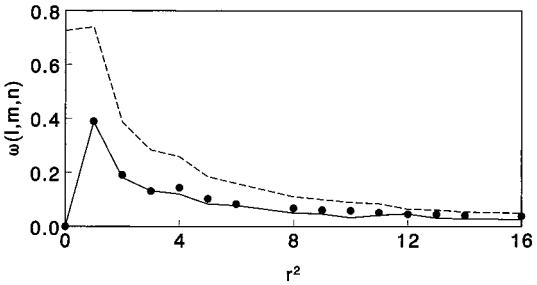

Figure 3. Caption as in Figure 1, but for 60-mers.

In Figure 1 it can be observed that at short radial distances, e.g., $r^2 \leq 6$, the ideal chain intramolecular distribution function is larger than that of the excluded volume chain (which was to be expected from the fact that single chains behave as self-avoiding walks). In the ideal chain, segments can fold back and several segments can occupy the same lattice site, making more compact conformations possible. This leads to a large residual correlation, i.e., $\omega^{intr}_{id}(0,0,0) - 1$ is nonzero and inevitably results in too high ω values at short distances. Since the summation of the intramolecular distribution function over all distances yields the total number of segments in the chain, the overestimated distribution at small distances must result in an underestimation of the distribution at larger distances. This is indeed observed in Figure 1. On the other hand, the excluded volume chain offers quite accurate predictions of the MC data. For the 16-mers the theoretical line for the intramolecular distribution function from the excluded volume chain passes through the MC data for all presented distances except at $r^2 = 4$. Note also that in agreement with the MC results $\omega^{intr}(0,0,0) - 1$ is identically zero.

In Figures 2 and 3 a comparison between MC simulation data and theory is presented for longer chain lengths; i.e., $s = 30$ and $s = 60$. Clearly, the predictions of the freely jointed chain for the intramolecular distribution deteriorates with increasing chain length (compare Figures 1−3). The predictions according to the excluded volume chain remain reasonably good for these chain lengths although also in this case the agreement between theory and simulation data is found to deteriorate with increasing chain length.

In Figure 4 the intramolecular distribution functions of 30-mers for two densities, $y = 0.00225$ and $y = 0.6865$

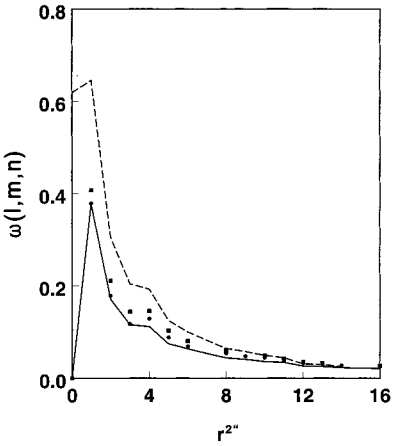

Figure 4. Intramolecular distribution function for 30-mers as a function of distance r^2 for different densities: $y = 0.00225$, (●); $y = 0.6865$, (■). Full line represents excluded volume theory and dashed line for freely jointed chain.

obtained from *NpT* MC simulations, are shown. The theoretical results for the ideal and excluded volume single chain distribution functions are also depicted by the dashed and solid lines, respectively. The theoretical distribution functions provide lower and upper bounds for the MC data. As already observed in Figures 1−3 the single chain intramolecular distribution function at zero density is quite successfully predicted by the excluded volume theory. When the density is increased, the MC intramolecular distribution for distance $r^2 \geq 1$ gradually shifts toward the ideal chain structure factor, indicating that the screening between intra- and intermolecular interactions indeed leads to more ideal chain behavior. However, the full ideal chain limit is never reached. In particular, the correlations at short distances are much smaller for the MC data than in the ideal chain ω^{intr} function. Although with increasing density the real chains tend to more ideal chain behavior, they always experience the short range excluded volume effects since two segments cannot occupy the same lattice site, i.e. $\omega^{intr}_{MC}(0,0,0) - 1 = 0$. From Figure 4 one might conclude that the excluded volume theory offers a reasonable prediction of the actual intramolecular distribution also at higher densities. In particular, if one is interested in properties involving short distances, the predictions of the excluded volume theory are better than those of the ideal chain model.

In Figure 5 the intermolecular correlations, calculated from the PRISM theory in combination with ω^{intr}_{id} (dashed lines) and ω^{intr}_{excl} (solid lines) are compared to MC simulation data for athermal chains ($u_{attr} = 0$) at 3 different densities, $y = 0.00455$, 0.0788, and 0.5383. Both theory and simulation show the well-known correlation hole, inside of which the concentration of monomers from other chains is reduced.[65] The predicted limiting zero-density intermolecular correlations are extremely poor irrespective of the intramolecular distribution function used. Similar discrepancies at low densities have already been found in off-lattice studies of short chain fluids[32] and small rigid molecules[24,25] and are related to the inexact limiting low density behavior of the (P)RISM theory.[33] Apparently, the use of a more accurate intramolecular distribution function for these low densities only results in a modest improvement. Clearly, the incorrect low density behavior of the PRISM theory is far more important. When the density is increased, the simulation data and the theoretical intermolecular correlations are in better agreement. Surprisingly, at the highest density shown here, the predictions using ω^{intr}_{id} are in excellent agreement at all distances. In line with the Flory ideality hypothesis, the ideal chain intramolecular distribution function captures quite accurately the correlations at large distances. But also at the short distances the predictions employing ω^{intr}_{id} are quite accurate and have the correct behavior at $(l,m,n) = 0$ which is a result of the exact closure condition $g(0,0,0) = 0$. At high density, the prediction of ω^{intr}_{excl} for the intermolecular correlations are not as accurate as those of ω^{intr}_{id}. The improvements found for the intramolecular distribution are not reflected in the intermolecular correlations.

The compressibility equation of state can now be obtained from the inter- and intramolecular correlations by numerical integration, presented in eq 16, or directly by eq 17. The latter equation only requires information about the final density. In Figure 6 the compressibility factor $\beta P v^* s/y$ is presented as a function of packing fraction y for athermal chains ($u_{attr} = 0$) with chain length $s = 20$ and $s = 30$. The solid circles and squares denote the MC simulation data for 20-mers and 30-mers, respectively. The dashed lines in Figure 6 are the result obtained from the lattice-PRISM theory in combination with ω^{intr}_{id}, and solid lines are obtained from

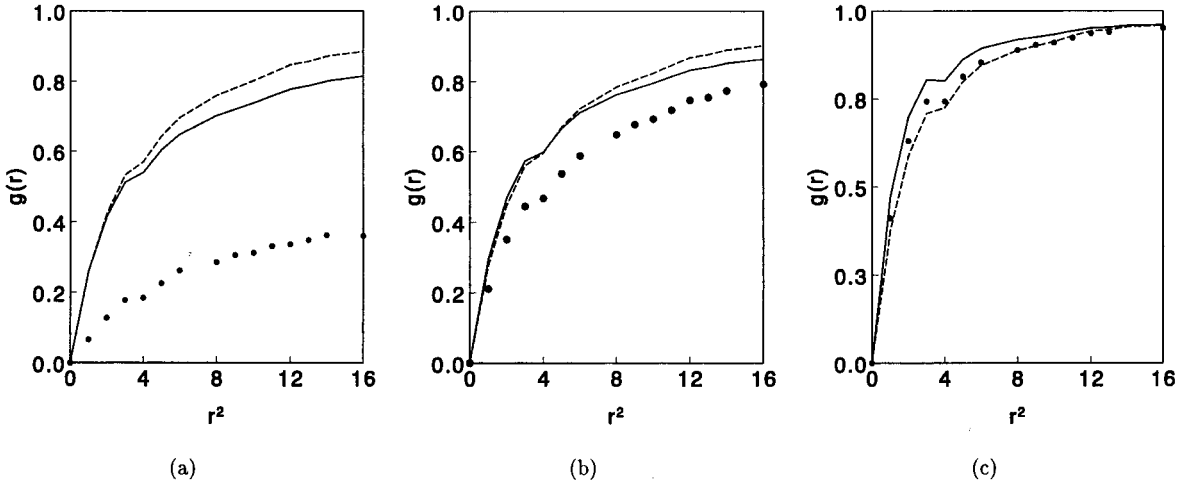

Figure 5. Intermolecular correlation function $g(r)$ as a function of distance r^2 at $s = 30$, $u_{attr} = 0$, and $y = 0.00455$, 0.0788, and 0.5383: MC simulations (●). Full line represents the excluded volume theory, and the dashed line depicts the results for freely jointed chains.

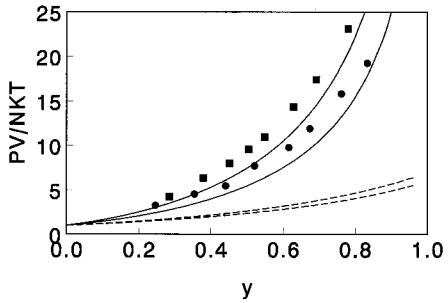

Figure 6. Compressibility factor as a function of packing fraction at $u_{attr} = 0$. MC simulations: $s = 20$ (●) and $s = 30$ (■). Full lines represent the excluded volume theory, and the dashed lines depict the results for freely jointed chains.

ω_{excl}^{intr}. The freely jointed chain model results severely underestimates the compressibility factor $\beta Pv^*s/y$ at all packing fractions. Moreover, at full packing, $y = 1$, the compressibility factor does not tend to infinity. From eq 16, we can appreciate that both the inter- and intramolecular correlations are important quantities for the EoS. At full packing of the lattice ($y = 1$) the total density of segments, given by $yG(l,m,n)$, equals unity for all distances. Hence, the compressibility is equal to zero and the compressibility factor tends to infinity at $y = 1$. However, the ideal chain model, allowing for nonphysical intramolecular overlap of segments, leads to a too high value of $\omega(l,m,n)$ at short distances. Consequently, the total density of particles (intra- and intermolecular) is larger than unity even at full packing and the compressibility becomes nonzero. This then results in a too small compressibility factor upon integration according to eq 17 or 18. On the other hand, the excluded volume theory, although approximate, accounts for these intramolecular excluded volume interactions and shows a largely improved limiting behavior at $y = 1$ for $G(l,m,n)$. This clearly results in a significantly improved agreement between theory and simulation.

In Figure 7 the intermolecular correlations for interacting 30-mers ($\beta u_{attr} = -0.2$) are presented. In these calculations the PRISM equation combined with ω_{id}^{intr} (dashed lines) or ω_{excl}^{intr} (solid lines) is solved using the MSA closure. It should be noted that the calculations for the interacting chains carry a certain inconsistency. The influence of the nearest neighbor interactions, contained in the closure relations, is only incorporated in the intermolecular correlations. For the intramolecular distribution function, the segmental interactions are assumed to be athermal. This inconsistency is not typical of the present discussion but is a consequence of the *a priori* treatment of intramolecular interactions independently of the intermolecular correlations. A self-consistent calculation of inter- and intramolecular correlations should provide an adequate remedy for this inconsistency. Despite this inconsistency, the theoretical variation with densities are quite similar to those observed for athermal chains and at low densities the PRISM predictions are particularly poor. However, also significant differences for these interacting systems are noticeable. At low and intermediate densities (parts a and b) the intermolecular correlations derived from the ideal chain model first reach a maximum at rather short distances before decreasing to the larger distance limiting behavior $g(r \to \infty) = 1$, in qualitative disagreement with the MC simulation data. Although less pronounced, the maximum is still present at the highest investigated density (Figure 7c). Calculations with the excluded volume intramolecular distribution function ω_{excl}^{intr} do not show the maximum in these interacting systems and the predictions using ω_{excl}^{intr} are much closer to the MC data at all densities. One can also observe that at high densities (compare Figures 7c and 5c) the intermolecular correlations for interacting and athermal systems are very similar. This is also correctly predicted by the PRISM/ω_{excl}^{intr} theory.

The equation of state for the interacting chains is depicted in Figure 8. The packing fraction is shown as a function of pressure for three values of the reduced interaction energy $\beta u_{attr} = 0, -0.45, -0.5$. Both in theory and simulation the density increases with pressure and reduced interaction energy. For the nonzero interaction parameters investigated here the theoretical prediction based on ω_{id}^{intr} (--) results in unphysical packing fractions larger than unity. Just as in the case of the athermal chains, the un physically large densities are related to the intramolecular segmental overlap still present in the ideal chain model. In addition, however, the intermolecular correlations, presented in Figure 7, result in an extra densification of the system. The theoretical prediction based on ω_{excl}^{intr} (—) leads to a correct physical behavior although the predicted densities are too low for all investigated pressures and nonzero interactions. For ω_{excl}^{intr} model the observed change in density with interaction energy is somewhat too small in comparison to the MC simulation data, whereas for ω_{id}^{intr} it is too large.

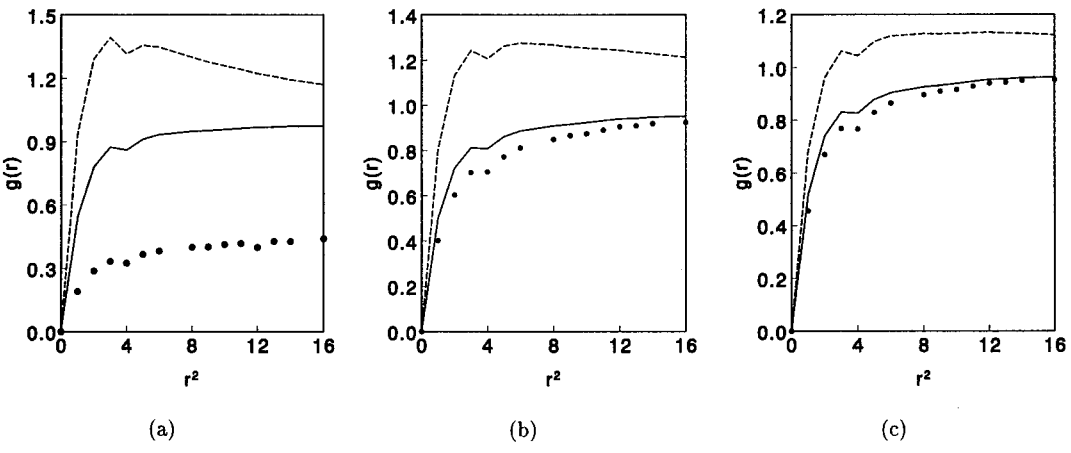

Figure 7. Caption as in Figure 5, but for $u_{attr} = -0.2$ and $y = 0.0043$, 0.294, and 0.5681.

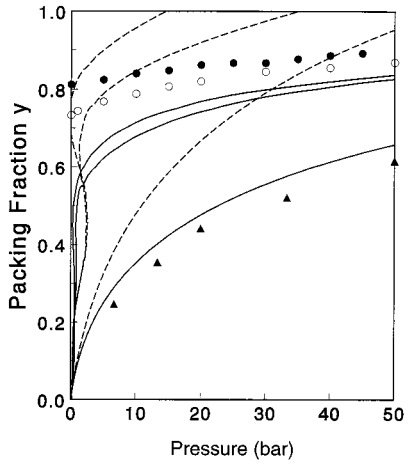

Figure 8. Density as a function of pressure for 30-mers and different interactions: $u_{attr} = 0$ (▲), -0.45 (○), and -0.5 (●). Full lines represent the ω_{excl}^{intr} with MSA; dashed lines represent the ω_{id}^{intr} with MSA.

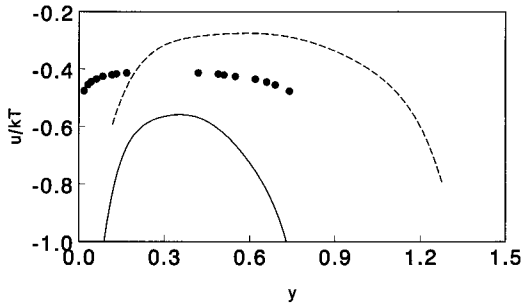

Figure 9. Liquid−vapor spinodal curves for 16-mers. Full lines represent the excluded volume theory; dashed lines represent the freely jointed chain model: (●) MC simulation for binodal curve.

Finally it can be observed that both the PRISM/ω_{excl}^{intr} and PRISM/ω_{id}^{intr} theoretical isotherms possess a van der Waals loop for sufficiently large attractive energies or low temperatures at low pressures. This is indicative of the vapor−liquid coexistence in this temperature and pressure region. The MC simulation data do not show this van der Waals loop. Further, it is not possible to locate the V−L coexistence gap with the *NpT* MC simulation algorithm employed in this study.[50] The coexistence gap can be investigated employing other simulation algorithms as demonstrated by Yan et al.[63,64]

The V−L binodal of a 16-mers obtained by Yan et al. is depicted in Figure 9. Together with the MC binodal data the liquid−vapor spinodal curves calculated according to the PRISM theory in combination with ω_{id}^{intr} and ω_{excl}^{intr} are presented for 16-mers. The finite size employed in the simulation makes it impossible to investigate the binodal curve down to lower temperature. Nevertheless, it is clear that the binodal curve tends to 0 K at $y = 0$ and $y = 1$. Spinodals and binodal are plotted as reduced interaction potential βu_{attr} vs packing fraction. The spinodal curve obtained from ω_{id}^{intr} is located at too high temperature and extends to packing fractions larger than unity. Again, the unphysical intramolecular overlaps of the ideal chain molecules lead to densities larger than one. The combination ω_{excl}^{intr}/PRISM produces an at least qualitatively correct spinodal curve. The maximum of the spinodal curve is known to be the critical state for a monodisperse lattice fluid. The estimated critical density $y_c \cong 0.34$ compares favourably to the critical density $y_c \cong 0.295$ estimated from the MC simulations. However, the total spinodal curve is shifted toward too low temperatures.

5. Conclusions

An intramolecular distribution function ω_{excl}^{intr} that accounts for the segmental overlaps related to the excluded volume of the flexible chain molecule has been derived by applying to lattice fluids diagrammatic techniques similar to those leading to the (P)RISM theory for the intermolecular correlations. Using this excluded volume intramolecular distribution function in the lattice-PRISM theory the intermolecular correlations for athermal and interacting chains have been calculated and the thermodynamic properties of the dense chain fluid have been studied. The theoretical results of the combinations lattice-PRISM/ω_{excl}^{intr} and lattice-PRISM/ω_{id}^{intr} have been compared to MC simulation data for the lattice model.

The intramolecular excluded volume theory compares favourably to the MC data for the single chain. On the other hand, the freely jointed chain model overestimates the single chain intramolecular distribution function at short distances and the quality of the predictions deteriorates with increasing chain length. When the density was increased, the MC intramolecular distribution function ω_{MC}^{intr} moves toward the freely jointed chain results, but even at the highest investigated densities, they are actually never reached. In fact, visual inspection of all results indicates that the new intramolecular distribution function ω_{excl}^{intr} in eq 13 yields a better prediction, especially at smaller distances, even at the highest investigated density.

By employment of the intramolecular distribution functions ω_{excl}^{intr} and ω_{id}^{intr} the intermolecular correlations for athermal and interacting chains at several densities have been calculated according to the lattice-PRISM theory. Intimately related to the inexact limiting behavior at low density of the PRISM theory, the predicted zero and low density intermolecular correlations are particularly poor. For athermal chains, the freely jointed chain model produces quite excellent predictions of the intermolecular correlation functions at higher density which is likely due to some effective cancellation of errors in theories used to produce the inter- and intramolecular correlations. For interacting chains the excluded volume theory produces better predictions for the intermolecular correlation functions for all investigated densities.

The compressibility factor of the athermal lattice fluid is underestimated by the freely jointed chain model and qualitatively incorrect and unphysical results are obtained due to the total neglect of intramolecular excluded volume. On the other hand, the combination lattice-PRISM/ω_{excl}^{intr} provides, at least, a qualitatively correct description of the equation of state properties when compared to the MC data. From off-lattice studies it has been found that the compressibility route to the equation of state is not the most accurate. For instance, Yethiraj et al. found some indications that the wall equation of state was closer to experimental data than, e.g., the compressibility and free energy "charging" routes.[61] However, irrespective of the relative success of the wall equation of state, the results are far from quantitative. Furthermore, previous lattice investigations have shown that the the wall equation of state is

not really preferable above, e.g., the compressibility equation of state.[66]

The liquid−vapor spinodal curve calculated for the freely jointed chain model is located at lower temperatures compared to the vapor−liquid coexistence curve obtained from MC simulations. Moreover, the spinodal curve extends to packing fractions larger than unity. The excluded volume theory offers a qualitatively correct spinodal curve. The maximum of the spinodal curve is known to be the critical state for a monodisperse lattice fluid. The estimated critical density $y_c = 0.34$ compares favourably to the critical density $y_c = 0.295$ estimated from the MC simulation results. However, the spinodal curve is shifted toward too high temperatures.

The single chain intramolecular distribution function ω_{excl}^{intr} can also be used in a study of polymer mixtures. In this case also the liquid−liquid miscibility behavior becomes of interest. This will be the subject of a future research.

Acknowledgment. S.W. wishes to acknowledge the financial support from the Netherlands Foundation of Chemical Research (SON). P.C. acknowledges partial support by VEGA2/4020/97.

Appendix A. The t_{ij}'s Calculated from Cluster Expansion

Curro, Blatz, and Pings have derived an approximation for the end point distribution function of an athermal chain in continuous space.[49] Here, we use this distribution function to calculate the intramolecular distribution function of an athermal chain on a cubic lattice. For an athermal chain the interaction potential of covalently and noncovalently bonded segments are given by eqs 2 and 3 with $u_{attr} = 0$. The total potential energy ϵ can be written as the sum of pair potentials between covalent bonds (w_{ii+1}) and noncovalent bonds (u_{ij})

$$\epsilon = \sum_{i=1}^{s-1} w_{ii+1} + \sum_{i=1}^{s-2}\sum_{j=i+2}^{s} u_{ij} \tag{A1}$$

The end point ($1 - s$) distribution function on the cubic lattice is given by

$$Z_{1s} = \sum_{l_{2...s-1}} \sum_{m_{2...s-1}} \sum_{n_{2...s-1}} \exp\left(\frac{-\epsilon}{kT}\right) \tag{A2}$$

Making use of eqs 2 and 3, the distribution function of an athermal polymer chain can be written as

$$Z_{1s}(r_{1s}) = \sum_{l_2,m_2,n_2} \cdots \sum_{l_{s-1},m_{s-1},n_{s-1}} \prod_{i=1}^{s-1} \delta(r_{ii+1} - 1) \times \prod_{i=1}^{s-2}\prod_{j=i+2}^{s} (1 - h_{ij}) \tag{A3}$$

with $h_{ij} = 1 - \exp(-\beta u_{ij})$. The $Z_{1s}(r_{1s})$ can be presented as a graph expansion with an expansion parameter λ. After manipulation the following expression is obtained:[49]

$$Z_{1s}(r_{1s};\lambda) = (1 + \lambda h_{1s}) \sum_{i=0}^{s-3/2} \xi_i(r_{1s})\lambda^i \tag{A4}$$

There are two types of graphs in $Z_{1s}(r_{1s};\lambda)$, i.e., nodal $N_{1s}(r_{1s};\lambda)$ and elementary graphs $E_{1s}(r_{1s};\lambda)$, such that

$$Z_{1s}(r_{1s};\lambda) = N_{1s}(r_{1s};\lambda) + E_{1s}(r_{1s};\lambda) \tag{A5a}$$

$$N_{1s}(r_{1s};\lambda) = \sum_{i=0}^{(s-1)/2} \nu_i(r_{1s})\lambda^i \tag{A5b}$$

$$E_{1s}(r_{1s};\lambda) = \sum_{i=1}^{(s-1)/2} \epsilon_i(r_{1s})\lambda^i \tag{A5c}$$

where $\nu_i(r_{1s})$ is the sum of nodal graphs with i loops in a chain of s subsystems and $\epsilon_i(r_{1s})$ is the sum of elementary graphs with i loops in a chain of s subsystems. In the theory of fluids an integral relation exists between the nodal and elementary graphs given by the well-known Ornstein−Zernike equation. Similarly, for the single chain excluded volume problem a ($s - 1$)th-order integro-differential equation exists

$$N_{1s}(r_{1s};\lambda) = \sum_{l_{s-1},m_{s-1},n_{s-1}} E_{1s-1}(r_{1s-1};\lambda)\delta(r_{s-1s} - 1) + \sum_{l_2,m_2,n_2} Z_{2s}(r_{2s};\lambda)\delta(r_{12} - 1) + \sum_{i_i,m_i,n_i i=3}^{s-2} E_{1i}(r_{1i};\lambda)Z_{is}(r_{is};\lambda) \tag{A6}$$

As in the integral equation theory of simple fluids, given another (approximate) relation between N_{1s} and E_{1s}, eq A6 can be solved and the distribution function Z_{1s} can be obtained. An approximation analogous to the Percus−Yevick approximation is invoked:

$$\epsilon_i(r_{1s}) \simeq h_{1s}\xi_{i-1}(r_{1s}), \quad i \geq 1$$

$$\epsilon_0(r_{1s}) = \xi_0(r_{1s}), \quad s = 2 \tag{A7}$$

$$\epsilon_0(r_{1s}) = 0, \quad s \geq 3$$

Combining eqs A4, A5, and A7 and putting $\lambda = -1$, the following equation results

$$E_{1s}(r_{1s};\lambda) = -\frac{h_{1s}}{H_{1s}} Z_{1s}(r_{1s};\lambda) \tag{A8}$$

where $H_{1s} = 1 - h_{1s}$.

Substitution of eqs A8 and A5 into eq A6 leads to

$$Z_{1s}(r_{1s}) = H_{1s}\left[\sum_{l_2,m_2,n_2} \delta(r_{12} - 1)Z_{2s}(r_{2s}) - \sum_{l_{s-1},m_{s-1},n_{s-1}} \frac{h_{1s-1}}{H_{1s-1}} Z_{1s-1}(r_{1s-1})\delta(r_{s-1s} - 1) - \sum_{i=3}^{s-2}\sum_{l_i,m_i,n_i} \frac{h_{1i}}{H_{1i}} Z_{1i}(r_{1i})Z_{is}(r_{is})\right] \tag{A9}$$

Equation A9 can be rearranged to

$$t_{1s}(r_{1s}) = \sum_{l_2,m_2,n_2} \delta(r_{12}-1)t_{2s}(r_{2s})H_{2s}(r_{2s}) - \sum_{l_{s-1},m_{s-1},n_{s-1}} h_{1s-1}(r_{1s-1})t_{1s-1}(r_{1s-1})\delta(r_{s-1s}-1) - \sum_{i=3}^{s-2}\sum_{l_i,m_i,n_i} h_{1i}t_{1i}(r_{1i})H_{is}t_{is}(r_{is}) \quad \text{(A10)}$$

with

$$t_{ij}(r_{ij}) = \exp\left(\frac{u_{ij}}{kT}\right)Z_{ij}(r_{ij}) = \frac{Z_{ij}(r_{ij})}{H_{ij}} \quad \text{(A11)}$$

Equation A10 is conveniently solved in Fourier space. For a homogeneous system, the lattice Fourier transform and its inverse are defined as

$$\hat{f}(k_l,k_m,k_n) = \sum_{l,m,n} f(l,m,n)\cos(lk_l)\cos(mk_m)\cos(nk_n) \quad \text{(A12a)}$$

$$f(l,m,n) = \left(\frac{1}{2\pi}\right)^3 \int_{-\pi}^{\pi}\int_{-\pi}^{\pi}\int_{-\pi}^{\pi} f(k_l,k_m,k_n)\cos(lk_l)\times \cos(mk_m)\cos(nk_n)\,\mathrm{d}k_l\,\mathrm{d}k_m\,\mathrm{d}k_n \quad \text{(A12b)}$$

Taking the Fourier transform of eq A10, an algebraic recurrent equation is obtained.

$$\hat{t}_{ij}(k_l,k_m,k_n) = 2\phi[\hat{t}_{ij-1}(k_l,k_m,k_n) - t_{i+1j}(0,0,0) - t_{ij-1}(0,0,0)] - \sum_{k=3}^{s-2} t_{1k}(0,0,0)[\hat{t}_{ks}(k_l,k_m,k_n) - t_{ks}(0,0,0)] \quad \text{(A13)}$$

where $\phi = \cos(k_l) + \cos(k_m) + \cos(k_n)$.

Successive applications of eqs A13 and A11 lead to the following results.

$$Z_{12}(r_{12}) = \exp(-\beta w_{12}(r_{12})) = \delta(r_{12}-1) \quad \text{(A14)}$$

Because the functions $t_{ij}(l,m,n)$ depend only on the difference in index of segments i and j, the $t_{ij}(l,m,n)$ can be written as $t_{l(l+i-j)}(l,m,n)$. For nearest neighbor segments l and $l+1$, the function $t_{ll+1}(r_{ll+1})$ and the Fourier transform are given by

$$t_{ll+1} = t_{12}(r_{12}) = Z_{12}/H_{12} = \delta(r_{12}-1) \quad \text{(A15)}$$

$$\hat{t}_{ll+1}(k_l,k_m,k_n) = 2[\cos(k_l)+\cos(k_m)+\cos(k_n)] = 2\phi \quad \text{(A16)}$$

$$\hat{t}_{ll+1}(0) = 6 \quad \text{(A17)}$$

$$t_{ll+1}(0) = \frac{1}{(2\pi)^3}\int_{-\pi}^{\pi}\int_{-\pi}^{\pi}\int_{-\pi}^{\pi} 2\phi\,\mathrm{d}k_l\,\mathrm{d}k_m\,\mathrm{d}k_n = 0 \quad \text{(A18)}$$

For next nearest neighbors l and $l+2$ we find

$$\hat{t}_{ll+2}(k_l,k_m,k_n) = \hat{t}_{13}(k_l,k_m,k_n) = 2\phi[\hat{t}_{23} - t_{23}(0) - t_{12}(0)] = 2\phi[\hat{t}(k_l,k_m,k_n) - 2t_1(0)] = 2\phi[2\phi - 0 - 0] = (2\phi)^2 \quad \text{(A19)}$$

$$\hat{t}_{ll+2}(0) = \hat{t}_{13}(0) = 36 \quad \text{(A20)}$$

$$t_{ll+2}(0) = t_{13}(0) = 6 \quad \text{(A21)}$$

For two segments l and $l+3$ separated by three bonds the results are

$$\hat{t}_{ll+3}(k_l,k_m,k_n) = \hat{t}_{14}(k_l,k_m,k_n) = 2\phi[\hat{t}_{24}(k_l,k_m,k_n) - t_{24}(0) - t_{13}(0)] = (2\phi)^3 - 24\phi \quad \text{(A22)}$$

$$\hat{t}_{ll+3}(0) = \hat{t}_{14}(0) = 72 \quad \text{(A23)}$$

$$t_{ll+3}(0) = t_{14}(0) = 0 \quad \text{(A24)}$$

For two segments separated by four bonds the t-function are

$$\hat{t}_{ll+4}(k_l,k_m,k_n) = \hat{t}_{15}(k_l,k_m,k_n) = 2\phi[\hat{t}_{25}(k_l,k_m,k_n) - t_{25}(0) - t_{14}(0)] - t_{13}(0)[\hat{t}_{35}(k_l,k_m,k_n) - t_{35}] = (2\phi)^4 - 18(2\phi)^2 + 36 \quad \text{(A25)}$$

$$\hat{t}_{ll+4}(0) = \hat{t}_{15}(0) = 684 \quad \text{(A26)}$$

$$t_{ll+4}(0) = t_{15}(0) = 18 \quad \text{(A27)}$$

For two segments separated by five bonds we obtain

$$\hat{t}_{ll+5}(k_l,k_m,k_n) = \hat{t}_{16}(k_l,k_m,k_n) = 2\phi[\hat{t}_4(k_l,k_m,k_n) - 2t_4(0)] - \sum_{i=3}^{4} t_{1i}(0)[\hat{t}_{i6}(k_l,k_m,k_n) - t_{i6}(0)] = (2\phi)^5 - 24(2\phi)^3 + 72(2\phi) \quad \text{(A28)}$$

$$\hat{t}_{ll+5}(0) = \hat{t}_{16}(0) = 3024 \quad \text{(A29)}$$

$$t_{ll+5}(0) = t_{16}(0) = 0 \quad \text{(A30)}$$

References and Notes

(1) Flory, P. J. *J. Chem. Phys.* 1942, *10*, 51.
(2) Huggins, M. L. *Ann. N.Y. Acad. Sci.* **1942**, *43*, 1.
(3) Flory, P. J. *Principles of Polymer Chemistry*; Cornell University Press: Ithaca, NY, 1953.
(4) Prigogine, I.; Bellemans, A.; Mathot, V. *The molecular theory of solutions*; North-Holland Publishing Co.: Amsterdam, 1957.
(5) Simha, R.; Somcynsky, T. *Macromolecules* **1969**, *2*, 341.
(6) Nies, E.; Stroeks, A. *Macromolecules* **1990**, *23*, 4092.
(7) Dickman, R.; Hall, C. K. *J. Chem. Phys.* **1988**, *89*, 3168.
(8) Sanchez, I. C.; Lacombe, R. H. *J. Phys. Chem.* **1976**, *80*, 2352.
(9) ten Brinke, G.; Karasz, F. E. *Macromolecules* **1984**, *17*, 815.
(10) Sanchez, I. C.; Balazes, A. C. *Macromolecules* **1989**, *22*, 2325.
(11) Freed, K. F. *J. Phys. A* **1985**, *18*, 871.
(12) Bawendi, M. G.; Freed, K. F.; Mohanty, U. *J. Chem. Phys.* **1986**, *84*, 7036.
(13) Bawendi, M. G.; Freed, K. F. *J. Chem. Phys.* **1988**, *88*, 2741.
(14) Pesci, A. I.; Freed, K. F. *J. Chem. Phys.* **1989**, *90*, 2003.
(15) Nemirovsky, A. M.; Bawendi, M. G.; Freed, K. F. *J. Chem. Phys.* **1987**, *87*, 7272.
(16) Freed, K. F.; Dudowicz, J. *J. Chem. Phys.* **1992**, *97*, 2105.
(17) Dudowicz, J.; Freed, K. F. *Macromolecules* **1991**, *24*, 5112.
(18) Curro, J. G.; Schweizer, K. S. *Macromolecules* **1987**, *20*, 1928.
(19) Schweizer, K. S.; Curro, J. G. *J. Chem. Phys.* **1988**, *89*, 3350.
(20) Schweizer, K. S.; Curro, J. G. *Macromolecules* **1988**, *21*, 3070.
(21) Curro, J. G.; Schweizer, K. S. *Macromolecules* **1991**, *24*, 6736.

(22) Janssen, R. H. C. Ph.D. Thesis, Eindhoven University of Technology, Eindhoven, The Netherlands, 1996.
(23) McQuarrie, D. A. *Statistical Mechanics*; Harper and Row Publishers: New York, 1976.
(24) Lowden, L. J.; Chandler, D. *J. Chem. Phys.* **1973**, *59*, 6587.
(25) Lowden, L. J.; Chandler, D. *J. Chem. Phys.* **1975**, *62*, 4246.
(26) Freasier, B. C. *Chem. Phys. Lett.* **1975**, *35*, 280.
(27) Jolly, D.; Freasier, B. C.; Bearman, R. J. *Chem. Phys. Lett.* **1977**, *46*, 75.
(28) Freasier, B. C.; Jolly, D.; Bearman, R. J. *Mol. Phys.* **1976**, *31*, 255.
(29) Tildesley, D. J.; Street, W. B. *Mol. Phys.* **1980**, *41*, 85.
(30) Aviram, I.; Tildesley, D. J. *Mol. Phys.* **1977**, *34*, 881.
(31) Chandler, D.; Andersen, H. C. *J. Chem. Phys.* **1972**, *57*, 1930.
(32) Yethiraj, A.; Hall, C. K.; Honnell, K. G. *J. Chem. Phys.* **1990**, *93*, 4453.
(33) Chandler, D. *J. Chem. Phys.* **1973**, *59*, 2742.
(34) Hsu, C. S.; Pratt, L. R.; Chandler, D. *J. Chem. Phys.* **1978**, *68*, 4213.
(35) Pratt, L. R.; Hsu, C. S.; Chandler, D. *J. Chem. Phys.* **1978**, *68*, 4202.
(36) Grayce, C. J.; Schweizer, K. S. *J. Chem. Phys.* **1994**, *100*, 6846.
(37) Grayce, C. J.; Yethiraj, A.; Schweizer, K. S. *J. Chem. Phys.* **1994**, *100*, 6857.
(38) Schweizer, K. S.; Honnell, K. G.; Curro, J. G. *J. Chem. Phys.* **1992**, *96*, 3211.
(39) Melenkevitz, J.; Schweizer, K. S.; Curro, J. G. *Macromolecules* **1993**, *26*, 6190.
(40) Melenkevitz, J.; Curro, J. G.; Schweizer, K. S. *J. Chem. Phys.* **1993**, *99*, 5571.
(41) Flory, P. J. *Statistical Mechanics of Chain Molecules*; Hanser Publishers: New York, 1989.
(42) Frenkel, D.; Smit, B. *Understanding Molecular Simulation from Algorithm to Applications*; Academic Press, Inc.: San Diego, CA, 1996.
(43) Cifra, P.; Karasz, F. E.; Macknight, W. J. *Macromolecules* **1992**, *25*, 4895.
(44) Cifra, P.; Karasz, F. E.; Macknight, W. J. *Macromolecules* **1992**, *25*, 192.
(45) The Gaussian chain consists of segments connected by bonds having a Gaussian distribution of bond length. In the freely jointed chain the segments are connected by constant bond lengths. The nonreversal random walk model introduces additional chemical details by forbidding back flipping.
(46) Wang, S. Ph.D. Thesis, Eindhoven University of Technology, Eindhoven, The Netherlands, 1997.
(47) Baxter, R. J. *J. Chem. Phys.* **1968**, *49*, 2770.
(48) Lomba, E. In *Supercritical Fluids*; Kiran, E., Levelt-Sengers, J. M. H., Eds.; Kluwer Academic Publishers: Dordrecht, The Netherlands, 1994; pp 1928−1931.
(49) Curro, J. G.; Blatz, P. J.; Pings, C. J. *J. Chem. Phys.* **1969**, *50*, 2199.
(50) Nies, E.; Cifra, P. *Macromolecules* **1994**, *27*, 6033.
(51) Chandler, D. In *Studies in Statistical Mechanics VIII*; Montroll, E. W., Lebowitz, J. L., Eds.; North-Holland: Amsterdam, 1982; p 275.
(52) Curro, J. G.; Schweizer, K. S. *J. Chem. Phys.* **1987**, *87*, 1842.
(53) Lebowitz, J. L.; Percus, J. K. *Phys. Rev.* **1966**, *144*, 251.
(54) Ballard, D. G.; Schelten, J.; Wignall, G. D. *Eur. Polym. J.* **1973**, *9*, 965.
(55) Cotton, J. P.; Decker, D.; Benoit, H.; Farnoux, B.; Huggins, J.; Jannik, G.; Ober, R.; Picot, C.; des Cloizeaux, J. *Macromolecules* **1974**, *7*, 863.
(56) Vacetello, M.; Avitabile, G.; Corradini, P.; Tuzi, A. *J. Chem. Phys.* **1980**, *73*, 543.
(57) Weber, T. A.; Helfand, E. *J. Chem. Phys.* **1979**, *71*, 4760.
(58) Koyama, R. *J. Phys. Soc. Jpn.* **1973**, *34*, 1092.
(59) Chandrasekhar, S. *Rev. Mod. Phys.* **1943**, *15*, 1.
(60) Prigogine, I.; Defay, R. *Chemical Thermodynamics*; Longmans Green and Co.: London, 1954.
(61) Yethiraj, A.; Curro, J. G.; Schweizer, K. S.; McCoy, J. D. *J. Chem. Phys.* **1993**, *98*, 1635.
(62) Janssen, R. H. C.; Nies, E.; Cifra, P. *Macromolecules* **1999**, *32*, 471.
(63) Yan, Q.; Liu, H.; Hu, Y. *Macromolecules* **1996**, *29*, 4066.
(64) Yan, Q.; Jian, J.; Liu, H.; Hu, Y. *J. Chem. Ind. Eng. (China)* **1995**, *46*, 517.
(65) de Gennes, G. *Scaling Concepts in Polymer Physics*; Cornell University Press Ltd.: London, 1979.
(66) Janssen, R. H. C.; Nies, E.; Cifra, P. *Langmuir* **1997**, *13*, 2784.

MA971381C